Probing Biomembrane Interfacial Potential and pH Profiles with a New Type of Float-like Fluorophores Positioned at Varying Distance from the Membrane Surface†

Ruud Kraayenhof,* Geert J. Sterk, and Harro W. Wong Fong Sang

Department of Molecular and Cellular Biology, Vrije Universiteit Amsterdam, De Boelelaan 1087, 1081 HV Amsterdam, The Netherlands

Received March 10, 1993; Revised Manuscript Received July 7, 1993•

ABSTRACT: Fluorophores of a new type were synthesized to probe the electrostatic potential or pH profiles in the external interface of biomembranes. The probes consist of the pH-sensitive fluorophore 7-hydroxycoumarin, coupled to a tetradecyl (myristyl) tail by a spacer group of varying length. A positively charged group is included between the tetradecyl and spacer groups to encourage a float-like alignment in the membrane head-group region. Three probes of this type were compared with 4-heptadecyl-7-hydroxycoumarin the fluorophore of which is embedded in the lipid head-group domain. Thus, a ruler-type positioning of the fluorophores was obtained at about 0.2, 0.6, 1.0, and 1.3 nm from the surface. The membrane-bound probes were tested in well-defined liposomes prepared by extrusion with different surface charge densities and size. The predicted positioning of the float-like probes is supported by their binding behavior in liposomes and by steady-state and nanosecond time-resolved fluorescence anisotropy, as well as by their accessibility to different quenchers. The interfacial electrostatic potential (ψ_d) and pH (pH_d) values were derived from the observed apparent pK_a shifts of the probes. The obtained ψ_d and pH_d profiles as function of the surface potential (ψ_0) and distance from the membrane surface are in good harmony with predictions from nonlinear Gouy–Chapman theory. The electrokinetic potentials (ζ) of the liposome series, measured by Doppler-electrophoretic frequency shift of laser light scattering, are in good proportion to the probe data. When bound to yeast cells, these probes monitor interfacial changes in parallel with glucose-induced medium acidification. Even in this poorly defined membrane system the derived ψ_d and pH_d values are in agreement with theoretical predictions. One of the new probes (U-6, d = 0.64 nm) is particularly suitable for applications in biomembranes because it can sense small ψ_d or pH_d changes in the physiological pH range. The chemical synthesis of U-6 with high yield and purity is described.

Biomembrane interfacial potential characteristics are of great significance for a variety of biomembrane-associated properties [for reviews, see McLaughlin (1977, 1989)]. Examples of these are the activity of membrane-bound enzymes (Krämer, 1989), membrane–membrane interactions (Rubin & Barber, 1980), peptide or protein import, bilayer lipid asymmetry (Hubbell, 1990), ion binding and translocation (Borst-Pauwels & Theuvenet, 1984), and biological energy transduction mechanisms (Kraayenhof et al., 1986).

Biomembranes generally bear a net negative charge leading to a higher proton and other cation concentration adjacent to their surface. Besides the negatively charged lipid head groups, acidic groups on membrane-bound proteins contribute to these interfacial charges, and it seems plausible to assume that such proteins mainly govern the dynamic properties of interfacial phenomena. For example, illumination or ATP hydrolysis induce a large and reversible increase of external negative surface charge density on chloroplast thylakoid membranes, as detected by free-flow electrophoresis and adsorption of cationic dyes (Schapendonk et al., 1980; Torres-Pereira et al., 1984). With highly stable ATP synthase proteoliposomes, reconstituted from thermophilic cyanobacterial components, kinetic discrimination of external and internal as well as interfacial and bulk H^+ displacements is possible (Van Walraven et al., 1984). Energy-linked surface charge rearrangements may initialize interfacial and bulk proton displacements in single-turnover and steady-state energization, respectively (Kraayenhof et al., 1986).

Direct measurement of electrostatic membrane potentials is only possible with free-flow particle electrophoresis methods, giving the electrokinetic or zeta (ζ) potential in the hydrodynamic plane of shear of the vesicles or cells at some distance from the membrane surface. These methods are useful for estimation of the surface potential (ψ_0) if this distance is known, but they are not sufficiently fast for monitoring interfacial changes in real time. The use of nonfixed dyes invariably meets with uncertainty about their exact location. The data obtained by these methods can only be compared with the real surface potential in well-defined artificial membrane systems with known surface charge density. Approaches using lipoid membrane-bound fluorescent probes (Montal & Gitler, 1973; Fromherz & Masters, 1974; Thelen et al., 1984; Teissié et al., 1985; Prats et al., 1986; Winiski et al., 1988; Soucaille et al., 1988; Fromherz, 1989) or covalently bound probes (De Kouchkovsky, 1975; Kraayenhof & Arents, 1977; Heberle & Dencher, 1992) offer the best alternatives to derive interfacial potential and pH values and, more interestingly, to monitor their time-resolved changes. Electron paramagnetic resonance probes are also powerful tools for measurements of interfacial potentials, even at macromolecular boundaries (Langner et al., 1990; Shin & Hubbell, 1992).

† This work was supported by the Netherlands Technology Foundation (STW) with financial aid from the Netherlands Organization for Scientific Research (NWO).

* Author to whom correspondence should be addressed.

• Abstract published in *Advance ACS Abstracts*, September 1, 1993.

0006-2960/93/0432-10057$04.00/0

The indirect information derived from molecular probes is significantly enhanced if a series of related probe derivatives is available which allows comparisons of responses as function of probe structure and location. The added value of this approach was convincingly demonstrated with the ruler-type of fluorophores (Waggoner & Stryer, 1970) and spin-labeled probes (Hubbell & McConnell, 1971) for studying the hydrophobic membrane domain at various depths.

The fluorescent aminoacridine atebrin (quinacrine), an uncoupler of photosynthetic energy transduction, was introduced as a probe for the "energized state" of choroplasts (Kraayenhof, 1970). Thereafter, a comparative study was conducted on a variety of aminoacridine analogues, including nonpermeable (polymer- or protein-bound) species, hydrophobically or covalently bound derivatives, and a spin-labeled fluorescent "double probe". It was concluded that the cationic aminoacridine probes predominantly interact electrostatically with the biomembrane surface charge (also forming dimers), rather than acting as direct ΔpH monitors by redistribution across the membrane [Kraayenhof & Arents, 1977; Kraayenhof, 1980; Torres-Pereira et al., 1984; see also Grzesiek and Dencher (1988)]. Two of the membrane-bound analogues, with their aminoacridine groups positioned at different distances from the membrane surface, showed different upward shifts of the apparent pK_a upon illumination of the chloroplasts, the largest shift being observed with the more closely bound probe. This preliminary observation suggested that a "calibration" of the interfacial potential would be feasible with more closely related probe analogues, a better fixed positioning normal to the membrane surface, and using better defined model membrane systems.

With this notion in mind we have synthesized a small family of umbelliferone (7-hydroxycoumarin)-based fluorescent probes, as a variation of the probes used by Fromherz (1973), but suited with a tetradecyl (myristyl) tail, a quaternary ammonium group, to fix the probe in a float-like position normal to the membrane, and a spacer group by which the distance between the fluorophore and the membrane surface is varied within the most interesting domain of the diffuse double layer, i.e., around 1 nm (Winiski et al., 1988; Langner et al., 1990). The responses of these probes are compared with the behavior of a related probe, 4-heptadecyl-7-hydroxycoumarin (U-2),[1] missing the spacer and anchoring groups and believed to have its fluorophore embedded in the lipid head-group domain (Fromherz, 1989; Pal et al., 1985).

In this paper we describe the ability of these fluorophores to probe the interfacial potential and pH values at varying surface charge density and distance in well-defined liposomes, prepared by the extrusion method (Mayer et al., 1986) from different mixtures of phosphatidylcholine (PC) and phosphatidic acid (PA). In addition, some results obtained with these probes in yeast cells are presented to demonstrate their use to monitor interfacial changes in a much less defined natural membrane system.

[1] Abbreviations: HEPES, *N*-(2-hydroxyethyl)piperazine-*N*'-2-ethanesulfonic acid; LUVETs, large unilamellar vesicles prepared by extrusion technique; PA, phosphatidic acid; PC, phosphatidylcholine; TPC, 2,2,5,5-tetramethyl-1-pyrrolidinyloxy-3-carboxamide; U-2, 4-heptadecyl-7-hydroxycoumarin; U-6, 4-[*N*,*N*-dimethyl-*N*-(*n*-tetradecyl)ammoniummethyl]-7-hydroxycoumarin chloride; U-10, 4-{2-[*N*,*N*-dimethyl-*N*-(*n*-tetradecyl)ammonium]ethylthiomethyl}-7-hydroxycoumarin chloride; U-13, 4-{4-[*N*,*N*-dimethyl-*N*-(*n*-tetradecyl)ammonium]butyl-(*N*',*N*'-dimethylammonium)methyl}-7-hydroxycoumarin dichloride.

EXPERIMENTAL PROCEDURES

Synthesis and Analysis of Fluorescent Probes. The simple synthesis procedure and the structural analysis of the three float-like probes are exemplified here for U-6. A solution of 4.2 g of *N*,*N*-dimethyl-*N*-(*n*-tetradecyl)amine (prepared from 1-bromotetradecane and dimethylamine), 3.7 g of 4-chloromethyl-7-hydroxycoumarin, and 5 mL of diisopropylethylamine in 50 mL of tetrahydrofuran was left at room temperature for 14 days. The formed white precipitate was filtered off, washed with tetrahydrofuran, and crystallized from a mixture of methanol and ethylacetate. The yield was as high as 60%. Melting point (Mettler FP 52 with microscope): 109–111 °C. ^{1}H NMR measurements (Bruker AC 200) yielded the following data: ^{1}H NMR (DMSO-d_6): 0.86 ppm, t, J = 6.3 Hz, 3.0 H (C–CH_3); 1.02–1.43 ppm, m, 22.0 H (C–C–$(CH_2)_{11}$–C); 1.63–1.90 ppm, m, 2.0 H (N–C–CH_2); 3.10 ppm, s, 6.0 H (2x N–CH_3); 3.41–3.62 ppm, m, 2.0 H (N–CH_2–C); 4.77 ppm, s, 2.0 H (coum–CH_2); 6.56 ppm, s, 1.0 H (coum–H_3); 6.79–6.98 ppm, m, 2.0 H (coum–H_5+H_6); 8.15 ppm, d, J = 8.7 Hz, 1.0 H (coum–H_8). High-resolution mass spectrometry (Finnigan MT 90; DCI, methanol): M+H found 452. Purity was also verified by reversed-phase thin layer chromatography (octadecyl r-p silica, Aldrich Z12,276-9) showing one spot with an R_f value of 0.78 in methanol. The synthesis of U-10 and U-13 proceeds principly the same, but the yields are much lower (about 12%). The structural analysis of U-10 by ^{1}H NMR was equally confirmative as for U-6 (data not shown), and high-resolution MS (FAB, glycerol) yielded 476 for M–Cl. Because U-13 was insoluble at the required high concentrations, NMR and MS analysis was not possible; TLC showed one spot with an R_f of 0.72 (methanol). The three float-like probes tested in this work were stable for at least 6 months, if stored in dry environment at room temperature. After storage of more than 1 year some decomposition (mainly U-10 and U-13) was evident from TLC. U-2, U-6, and U-10 were dissolved before use in ethanol, U-13 in DMSO, at concentrations of maximally 5 mM.

The structures and space-filling models of the synthesized compounds and of U-2 are depicted in Figure 1. The average distance between the coumarin hydroxyl group of the float-like probes and the membrane surface was derived using a molecular modeling program (Chem3D Plus, Cambridge Scientific Computing Inc., London, U.K.), accounting for some flexibility of the spacer groups, and assuming alignment of the tetradecyl-bound quaternary nitrogen atom with the lipid phosphoryl groups in the plane of the membrane, defining this alignment plane as distance zero. The position of the U-2 fluorophore will be explained under Discussion.

Preparation of Liposomes. Purified phosphatidylcholine (PC) and phosphatidic acid (PA) were kindly provided by Dr. B. de Kruijff. Commercially available lipids (Sigma) were also used. Purity was verified by TLC. LUVETs of different PC/PA mixtures were prepared by mixing the lipid solutions (5 mg·mL^{-1}) in chloroform/methanol (9:1), rotational evaporation of the solvent until dryness, vortex mixing, and 10 freeze–thaw cycles of the suspension in 10 mM KCl, 2 mM HEPES buffer, pH 7.4 (standard medium), and stepwise extrusion of the multilamellar vesicles as described by Mayer et al. (1986). The extrusion procedure involved, successively, five cycles through 800-nm pore polycarbonate membranes (Nuclepore, Costar Europe Ltd.) and 10 cycles through 400-nm pore membranes. The 400-nm LUVETs were used for most experiments. For studying the effects of vesicle size,

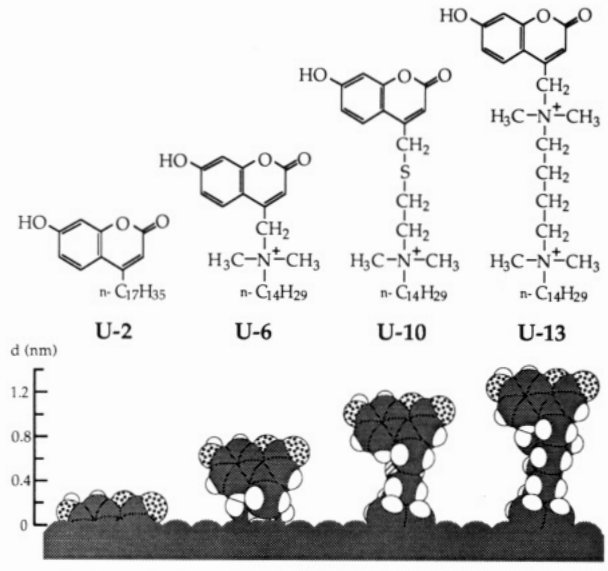

FIGURE 1: Chemical structures of the synthesized (U-6, U-10, U-13) and commercially available (U-2) fluorescent probes and space-filling models of their assumed position in the membrane–medium interface. Estimated average distances between the coumarin-hydroxyl groups and the plane through the tetradecyl-bound quaternary ammonium groups are 0.15, 0.64, 1.02, and 1.30 nm, respectively.

additional extrusion cycles through 200-, 100-, and 50-nm pore membranes (10 cycles each) were performed. For each LUVET preparation fresh polycarbonate membranes (in stacks of two) and polyethylene supporting filters (36 μm pores, thickness 2.5 mm) were used. The presented experiments were carried out with LUVETs prepared on the same day. Lipid contents were determined by phosphorus analysis after destruction according to Rouser et al. (1975).

Probe Binding Experiments with LUVETs. LUVET preparations were diluted to 0.1–0.25 mg lipid·mL^{-1} in 2 mL of standard medium and incubated for 30 min at room temperature with 0, 5, 10, or 20 μM fluorescent probe under stirring. Probe binding was measured fluorimetrically after gel filtration of the liposomes by the column-centrifugation procedure, essentially as described by Penefsky (1979). Disposable 5-mL syringes were fitted with 13-mm diameter polyethylene disks (36-μm pores, thickness 2.5 mm) and filled with 2.5 mL of preswollen Sephadex G-50 fine (Pharmacia). The columns were placed in 10-mL tubes, precentrifuged (MSE Chilspin, 2 min at 1000 rpm), and washed twice with 2 mL of the same medium before 2 mL of the probe–liposome mixtures was added and centrifuged. Binding was calculated from the fluorescence signals of the samples and of control runs (without liposomes or probes) and calibrations in each liposome type.

Doppler-Electrophoretic Light Scattering Analysis. The ζ potentials derived from the electrophoretic mobilities and the average hydrodynamic vesicle diameters of different liposome preparations were obtained with a DELSA 440 apparatus (Coulter Electronics, Inc., Hialeah, FL) which employs a four-angle detection of the Doppler shift of frequency of scattered laser light. The apparatus also measures the electric conductance of the medium and applies the data in calculations. Medium viscosity was checked separately with a Schott (Mainz, FRG) apparatus.

Calculations and Simulations. The calculation of the charge densities of LUVETs was based on the assumptions that both PC and PA molecules (fully hydrated) occupy a surface area of 70 Å^2 and that PA bears 1.17 electronic charge at pH 7.4 (cf. Träuble & Eibl, 1974). The corresponding surface potential (ψ_0) calculations were based on the Gouy equation (cf. McLaughlin, 1977). From the adsorption of K^+ ions (relative to that of Li^+, Na^+, and Cs^+) to the LUVETs (cf. Eisenberg et al., 1979; Ermakov, 1990) the estimated association constant was 1.6 ($\pm$ 0.5) M^{-1} (at 10 mM), and the ψ_0 values were corrected accordingly (see Discussion). The local electrostatic potential at distance d from the membrane surface (ψ_d), i.e., at the level of the coumarin-hydroxyl groups of the probes, is calculated from the difference of the apparent pK_a values with those at (extrapolated) zero surface charge density (pK_a^0), also corresponding to the difference between local pH (pH$_d$) and bulk medium pH (pH$_b$), according to the relation [adapted from Davies and Rideal (1963), and Fromherz (1989)]:

$$\psi_d = -2.3RT/F(pK_a - pK_a^0) = -2.3RT/F(pH_b - pH_d)\ \text{mV}$$

in which $RT/F = 25.69$ mV at 25 °C (cf. McLaughlin, 1977). The theoretical ψ_d (and pH$_d$) profiles were simulated by a spreadsheet protocol, using the equations for the Gouy–Chapman theory, based on the nonlinear Poisson–Boltzmann relation (McLaughlin, 1977).

Fluorescence Measurements. Fluorescence spectra and measurements of intensity, quenching, and steady-state fluorescence anisotropy were recorded with a SLM-Aminco SPF-500 fluorescence spectrophotometer in calibration mode. The fluorimetric determinations of the pK_a values of the membrane-bound probes were performed by acid–base titrations in the standard medium. During titrations the medium pH was monitored with a fast-responding solid-state micro-pH electrode (Lazar Research Laboratories, Inc., Los Angeles, CA), accurately calibrated with standard buffers. Titrations were started at the low-pH end and were performed as fast as possible. For those cases where the titration end values showed increased scattering (at very high pH), simulated titration curves were fitted through the data that were accurate. We have also employed the alternative method suggested by Fromherz (1989) to determine the pK_a values from the ratios of the dissociated and undissociated probe contributions to the excitation spectra.

Fluorescence lifetime and anisotropy decay measurements were performed with a laboratory-built instrument, based on direct read-out of the fluorescence transients induced by repetitive laser excitation at 10–50 Hz pulse frequency. The pulsed dye laser was a Dyescan 2100 (EG&G Princeton Applied Research, Princeton, NJ). For excitation of the probes at 370 nm, the laser dye BBQ (Radiant Dyes Chemie, Wermelskirchen, FRG) was used; in some experiments the nitrogen pump laser output was directly applied. The measuring cuvette was as earlier described (Kraayenhof et al., 1982) but modified to allow a T-configuration for dual-polarized emission detection and the use of conical lenses (Rigler et al., 1974). The two polarized emission beams were passed through beam scramblers and Jobin-Yvon H10 monochromators and detected by cooled Philips PM2254B photomultipliers. The signals were passed into an EG&G/PAR 4400 boxcar signal-processing system.

In fluorescence quenching experiments corrections were applied for changes in ionic strength (Lakowicz, 1986). In the case of iodide, 10 mM $Na_2S_2O_4$ was added to keep the iodide in its reduced form. In the case of thallium, the KCl in the standard medium was replaced by 10 mM KNO_3; Tl(I) was added as the nitrate and the control series contained the corresponding KNO_3 concentrations. All fluorescence experiments were carried out at 25 °C.

Experiments with Yeast Cells. Fresh baker's yeast paste of *Saccharomyces cerevisiae*, strain CBS 6131 (Gist-Brocades, Delft, The Netherlands), was suspended in 25 mM KCl, 25 mM NaCl, and 2 mM HEPES buffer, pH 7.2, at a concentration of 5% (w/v), and starved for at least 4 h under vigorous shaking at 25 °C. Probe (5 μM; about 5 nmol per mg of yeast protein) was added, followed by two centrifugation–washing steps. The probe pK_a values were measured at 25 °C in the absence and presence of 20 mM Mg^{2+}, which is supposed to rather effectively screen the membrane surface charge. The fluorimetric determinations of the bound probe pK_a values by 50 mM glucose-induced "self titrations" always started at the high-pH end. By short preincubation at this higher pH (8.5–9.5), the cell walls appeared to partly disrupt and become freely permeable toward bromophenol blue, as microscopically observed. For the purpose of these experiments it was not considered necessary to remove cell wall fragments since their presence does not affect the predominant binding of dyes to the plasma membrane (Theuvenet et al., 1984). The average ζ potential of yeast cell populations was determined with a micro free-flow electrophoresis apparatus (Rank Brothers, Mark II, Cambridge, U.K.).

Chemicals. All chemicals were of analytical grade. 4-Heptadecyl-7-hydroxycoumarin (U-2) and 4-chloromethyl-7-hydroxycoumarin were obtained from Molecular Probes, Inc., Eugene, OR (the latter compound was also synthesized by us); 2,2,5,5-tetramethyl-1-pyrrolidinyloxy-3-carboxamide (TPC) was obtained from Eastman Kodak Co., New Haven, CT, and thallium(I)nitrate from Merck, Darmstadt, FRG.

RESULTS

Selection of Probes. The three float-like fluorescent probes presented in this work were chosen from various series of synthesized and tested probes. A single tetradecyl chain was chosen for the tail group, because it appeared that this substitution to umbelliferone and 9-amino-substituted acridines caused much less uncoupling of chloroplast energy transduction than those containing longer hydrocarbon chains (R. Kraayenhof, unpublished). A positively charged quaternary ammonium group was introduced on top of this tail in order to encourage a stable float-like positioning normal to the membrane surface by electrostatic interaction with the negative phosphoryl groups. We found that increasing the spacer length beyond that of U-13 by adding a third (butyl-spaced) quaternary ammonium group ("U-18", fluorophore at about 1.8 nm) led to extensive liposome aggregation after addition of the probe. This is probably caused by electrostatic interaction of the uppermost positive groups with other liposomes. Thus, the range of useful ruler-type measurements seems to be limited with the present series of related probes. In addition to the three synthesized probes, we have tested 4-heptadecyl-7-hydroxycoumarin (U-2). This probe positions its fluorophore between the lipid head groups (Fromherz, 1973, 1989; Pal et al., 1985) and may serve as a reference for the relative positioning of the exposed float-like probes.

Binding of Float-Like Probes to LUVETs. The binding of U-6 to liposomes, extruded through 400-nm pores (for real sizes, see Table I) and with increasing surface charge (% PA of total lipid), is shown in Figure 2. The binding shows saturation rather than partitioning characteristics (Figure 2A) and is progressively increased with increasing negative surface charge density (Figure 2B). The binding behavior of U-10 and U-13 is very similar to that of U-6 (data not shown). This supports the notion that apart from the strong hydrophobic interaction of the tetradecyl chain, the adjacent quaternary ammonium group interacts electrostatically with the phosphoryl groups of PA, and that these probes may indeed be positioned as illustrated in Figure 1. U-2 and other 4-alkylumbeliferones show typical partitioning behavior in PC liposomes and detergent micelles with extremely high distribution coefficients (Fromherz, 1989). We have confirmed this and observed linear binding curves (not shown), both in pure PC liposomes and 10% PA liposomes.

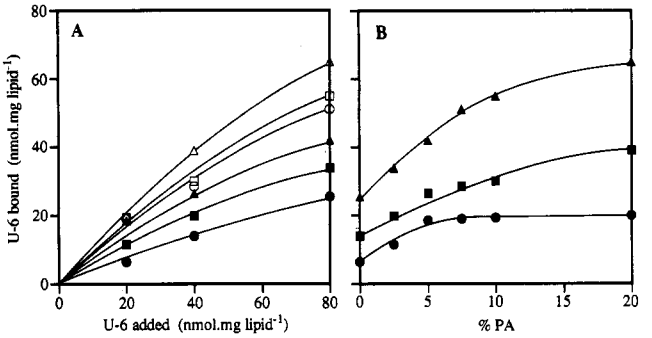

FIGURE 2: Binding of the fluorescent probe U-6 to LUVETs with different charge densities as function of added probe (A) and of weight percentage of mixed PA (B). The LUVETs used were extruded through 400-nm pores (see Table I for real sizes). For experimental details see Experimental Procedures. In panel A binding was measured at PA fractions of 0 (●), 2.5 (■), 5 (▲), 7.5 (○), 10 (□), and 20% (△). In panel B the U-6 concentrations were 20 (●), 40 (■), and 80 (▲) nmol·mg of lipid^{-1}.

The pure PC liposomes also show appreciable binding of the float-like probes. This is probably due in part to a small net negative charge of PC at pH 7.4 [see also measured ζ potential in Table I and Makino et al. (1991)].

Figure 2 also shows that, at 20 nmol U-6·mg of lipid^{-1}, corresponding to a molar probe/lipid ratio of about 1:62, more than 90% of the probe is already bound at a PA fraction of 5%, i.e., at a probe/PA ratio of about 1:3. For the case of U-13 this implies that there is no extra contribution to the binding by the second ammonium group on top of the spacer. Binding kinetics for U-2 in liposomes showed a halftime of about 2 min, but full equilibration took at least 20 min. Binding of the float-like probes is complete within 3–6 min. In all cases a standard incubation time of 30 min was maintained.

In further experiments a molar ratio probe/total lipid of 1:165 is used for all probes (2 μM probe, 0.25 mg of lipid·mL^{-1}) or less. At this probe/lipid ratio we observed no significant effect on the ζ potential (data not shown), and the fluorescence signal/noise ratio in the liposome suspensions is still sufficiently high. It should be noted that the overall probe fluorescence signal is decreased (by 50–70%) in the presence of the fairly turbid liposomes.

Particle size measurements indicated that the four probes form large micelles (350–650 nm) when added to the standard medium, which also becomes visibly turbid. However, in the presence of liposomes and with the low probe concentrations used, size measurements with the DELSA technique did not reveal different particle sizes from those of liposome preparations without probes. This was also confirmed by electron micrographs of negatively stained liposomes with or without probes (not shown). It is therefore unlikely that substantial fractions of probes reside in separate or liposome-bound micelles (see also Discussion).

Fluorescence Anisotropy and Fluorescence Quenching Experiments. Additional support for the proposed positioning of the float-like probes in the membrane is provided by fluorescence anisotropy and fluorescence quenching measurements. Figure 3 shows the steady-state anisotropy (r_s)

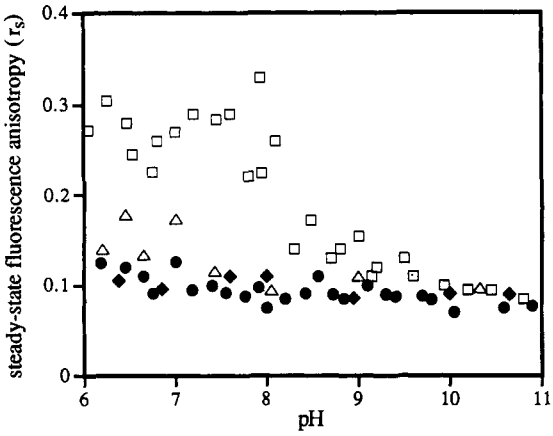

FIGURE 3: Steady-state fluorescence anisotropy (r_s) of probes as function of medium pH. The standard medium contained 400-nm/10% PA liposomes, 0.5 mg lipid·mL^{-1}, and 2 μM probe. (□) U-2; (●) U-6; (△) U-10; (◆) U-13.

values of the four probes, bound to 400-nm/10% PA LUVETs, as function of medium pH. At pH 7.4 the U-2 fluorophore apparently resides in a more constrained position than those of the three float-like probes. Similar r_s values for U-2 were observed in other liposome systems by Pal et al. (1985). Interestingly, the r_s value for U-2 was found to decrease above a pH of about 8 to the low values observed for the other probes. This pH effect is not due to ionization of the coumarin hydroxyl group since its pK_a is already shifted to a value around 10 after binding to these liposomes (Table I, upper panel). The other probes do not show this pH dependency although their pK_a values after binding are within the critical pH range. The pH effect can be explained by the dissociation of the second ionizable group on PA [cf. Figure 3 in Träuble and Eibl (1974)], inducing a transition to a more fluid phase and allowing increased rotational freedom of the U-2 fluorophore. In Figure 4 the nanosecond time-resolved fluorescence transients induced by the excitation pulse and the derived anisotropy decays are shown for U-2 and U-6. Figure 4A shows the raw experimental transients of the parallel ($I_\parallel$) and perpendicular ($I_\perp$) emission components of U-2 and U-6 at pH 7.4, together with the instrumental pulse response (P), measured on the liposomes without probe (same results found with a suspension of 300 nm latex spheres) and with the emission monochromator set at the excitation wavelength. From reconvolution least-squares analysis of total emission intensity ($I_\parallel + 2I_\perp$) and P we have determined the fluorescence lifetimes (τ) of the membrane-bound probes. For U-2, τ-values were 5.76 and 5.52 ns at pH 7.4 and 8.9, respectively; for U-6, the corresponding values were 4.88 and 4.67 ns, respectively (sd $\cong$ 0.5 ns in all cases). Thus, τ is not significantly changed with the type of probe and with pH rise. It was earlier reported that the fluorescence lifetime of U-2 is not affected by environmental changes (Pal et al., 1985; Fromherz, 1989). Therefore, this parameter is not a suitable indicator for the different positions of the fluorophores. In Figure 4B the fluorescence anisotropy decays (r_t) are depicted. All decays can be satisfactorily fitted to single exponential kinetics. U-2 displays typical hindered fluorophore behavior at pH 7.4. Its initial anisotropy (r_0) reaches the theoretical maximum of 0.4, and there is a clear limiting anisotropy (r_∞) of 0.15 at pH 7.4. At pH 8.9 U-2 experiences more rotational freedom: r_0 = 0.24 and r_∞ = 0.07. The rotational correlation times (Φ), determined from the transients (cf. Lakowicz, 1986) are 12.2 and 6.5 ns, at pH 7.4 and 8.9, respectively. For U-6 the r_0 values are also lower at both pH values, and Φ = 5.4 and 4.3 ns at pH 7.4 and 8.9, respectively. These results clearly indicate that the fluorophore of U-6 with the shortest possible spacer already experiences much more rotational freedom than U-2 at pH 7.4.

The accessibility of the membrane-bound probes to three different fluorescence quenchers was studied. Iodide (I^-), thallium(I) (Tl^+), and the uncharged amphiphilic nitroxyl free radical TPC were tested in standard medium (pH 7.4), and the results are presented as Stern–Volmer plots in Figure 5. The good linearity of these plots indicates the occurrence of single fluorophore populations, accessible to the quenchers, although to different extents. The membrane-embedded U-2 is much less accessible to I^- and Tl^+ than U-6 and U-10. However, at pH 8.9 its accessibility to Tl^+ is increased (Figure 5B, dashed line), in agreement with the high-pH effect on its fluorescence anisotropy. It should be noted that the negative membrane surface charge increases the local concentration of cationic quenchers by their attraction and thereby enhances their effect. Conversely, it attenuates the effects of anionic quenchers by their repulsion. Therefore, true efficiencies of quenching are not derived here. The more lipophilic TPC collides more easily with U-2 than the ionic quenchers, as expected. Since the bimolecular quenching constant may vary for each probe–quencher combination, we have also compared the quenching effects with the probes suspended in the standard medium without membranes, assuming similar accessibilities in this case. These controls showed that U-2 and U-6 were quenched with equal efficiency (at lower concentrations than in Figure 5) and U-10 with slightly lower efficiency by I^- and TPC. We conclude that the quenching experiments do not discriminate between the positions of the float-like probes but clearly demonstrate different accessibilities between the latter and the more occluded U-2.

Fluorescence Spectra. The calibrated fluorescence excitation and emission spectra of U-6 bound to 400 nm/2.5% PA LUVETs at different medium pH are pictured in Figure 6. The acidic and basic forms have excitation maxima at 323 and 365 nm, respectively, and a common emission maximum at 465 nm. The spectra of U-13 are very similar. U-10 shows a more complicated behavior. Its excitation maxima are at 327 and 385 nm, respectively, and its emission maximum shifts upon protonation from 465 to 453 nm. At increasing surface charge density of the liposomes the excitation spectra of all probes assume the more acidic forms and higher apparent pK_a values, as expected (not shown).

Apparent pK_a Values of Bound Probes. After binding of the probes to LUVETs with different charge densities (% PA weight fraction) and size, their apparent pK_a values were determined by fluorimetric titrations (Table I). The upward shifts of the apparent pK_a values upon binding to increasingly negative LUVETs are in agreement with earlier experiments with 4-alkyl-7-hydroxycoumarins in micelles and bilayer membranes (Fromherz, 1973; Fernández & Fromherz, 1977). Although the pK_a changes are rather small, especially with U-10 and U-13, the measurements were remarkably reproducible (SD 0.06–0.13, 5–9 experiments) within the same batch of LUVETs and avoiding prolonged incubation in the high-pH range. For comparison 100% PC/0% PA liposomes were also tested. At pH 7.4 these liposomes appeared to have non-zero ψ_0 and ζ potentials [see also Schlieper et al. (1981) and Makino et al. (1991)]. From these published data and our ζ potential measurements, we estimated a ψ_0 of −10.3 mV. The calculated ψ_0 values for the different PC/PA liposomes (Table I) were accordingly corrected. These ψ_0 values are also corrected for K^+ adsorption (see Experimental Procedures); if K^+ adsorption is ignored, the values range from

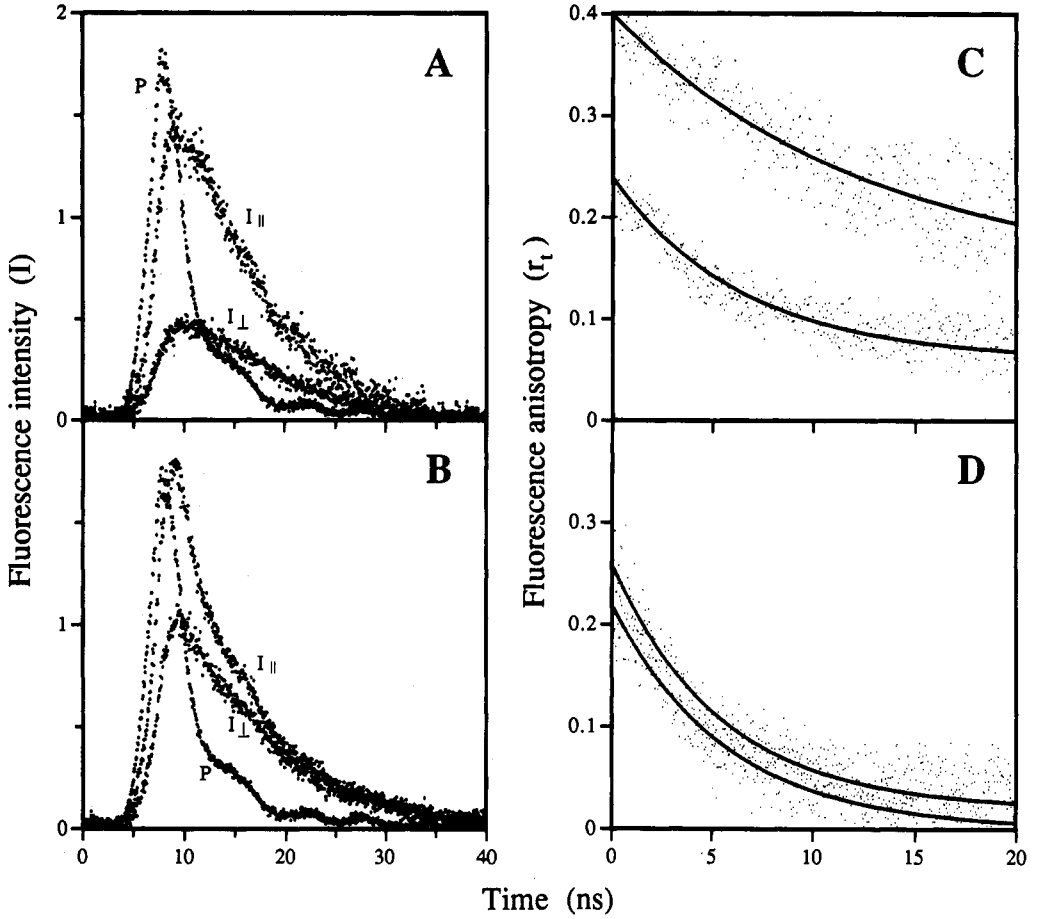

FIGURE 4: Time-resolved fluorescence transients of U-2 (A) and U-6 (B) at pH 7.4 and fluorescence anisotropy decays (r_t) of U-2 (C) and U-6 (D) at pH 7.4 and 8.9. In panels A and B the raw experimental data (six sweeps of 50 ns each; sampling time, 5.12 min) of the parallel ($I_{||}$) and perpendicular ($I_{\perp}$) emission components and the instrumental pulse response (P) are shown. $I_{\perp}$ responses were corrected for the G factor (=1.1). In panels C and D single-exponential fits of the anisotropy decays are depicted: upper curves in both panels at pH 7.4, lower curves at pH 8.9. Conditions are as given in the legend to Figure 3.

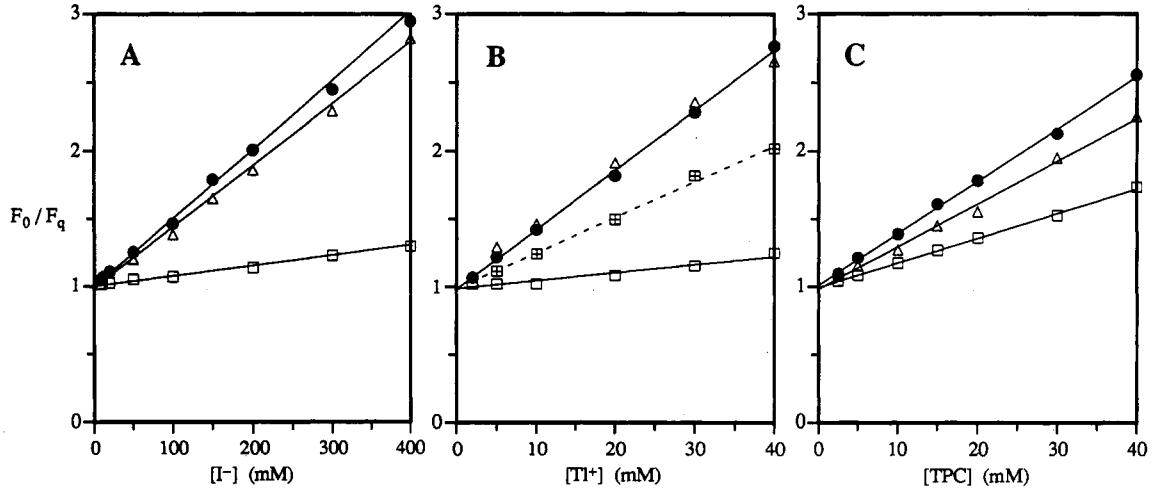

FIGURE 5: Relative efficiency of probe fluorescence quenching by iodide (A), thallium (B), and TPC (C). Probe and lipid concentrations in standard medium, pH 7.4 (in B U-2 also tested at pH 8.9), were as in Figure 3 (see also text). Corrections were applied as indicated under Experimental Procedures. F_0, initial fluorescence signal; F_q, quenched fluorescence. (□) U-2, pH 7.4; (⊞) U-2, pH 8.9; (●) U-6, pH 7.4; (△) U-10, pH 7.4.

about −11 to −122 mV. The use of a series of similar liposomes with increasing ψ_0 allows the determination of the pK_a^0 values for the probes at vanishing surface potential by extrapolating the obtained data to $\psi_0 = 0$. The pK_a^0 values for U-2, U-6, U-10, and U-13 determined by this method were found to be 8.74, 6.94, 8.44, and 7.49, respectively. We prefer this method over assuming a "standard" pK_a^0 value measured in a different system like Triton X-100 micelles, as suggested by Fromherz (1989). For U-2 our pK_a^0 value is not much different from that obtained by Fromherz in Triton X-100 (8.80). However, in the case of U-6 we observed a much higher value in 2 mM Triton X-100 (8.25). The pK_a of U-6 in 10% ethanol is 7.75 [the same as for 7-hydroxycoumarin in water, cf. Montal and Gitler (1973)]. Similar deviations were observed with U-10 and U-13 in these media. The different structural features of the float-like probes as compared to the 4-alkyl-7-

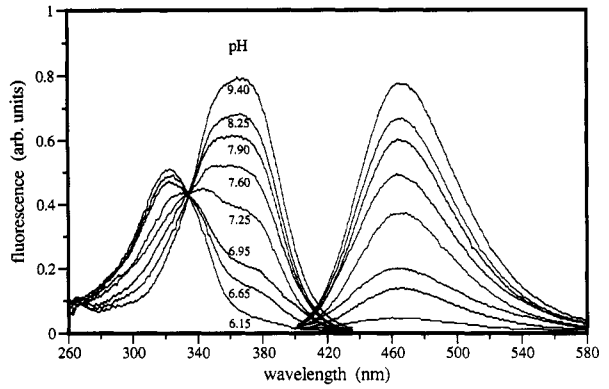

FIGURE 6: Fluorescence excitation and emission spectra of U-6, bound to LUVETs. The standard medium contained 400-nm/2.5% PA liposomes at different medium pH, as indicated. The concentration of bound U-6 was 8 nmol·mg of lipid^{-1}. Excitation and emission wavelength settings were 365 and 465 nm, respectively. The fluorimeter was set in the calibration mode.

Table I: Measurements of the Apparent pK_a Values of Fluorophores Located at Various Distances from the Membrane Surface, the Electrokinetic Potentials (ζ), and Average Hydrodynamic Diameters of Well-Defined Liposomes, Prepared with Different Surface Charge Density and Size[a]

liposomes		electrostatic potentials		apparent pK_a of bound probes			
PA fraction (%)	size (nm)	ψ_0 (mV)	ζ (mV)	U-2	U-6	U-10	U-13
0	394	−10.3[b]	−7.2	8.89	7.08	8.55	7.57
2.5	379	−36.2	−23.8	9.32	7.42	8.85	7.83
5	355	−54.6	−40.9	9.61	7.67	9.03	7.95
7.5	340	−67.3	−47.8	9.80	7.79	9.23	8.10
10	294	−76.3	−54.2	10.10	7.91	9.28	8.16
20	255	−96.3	−72.2	10.35	8.08	9.32	8.27
10	179	−76.3	−50.4	–[c]	7.73	–	–
10	75	−76.3	−51.1	–	7.62	–	–
10	–	−76.3	−48.9	–	7.50	–	–

[a] In the upper section the final extrusion pore size was 400 nm; in the lower section final pore sizes were 200, 100, and 50 nm, respectively. For calculation of ψ_0 and measurements of ζ and average hydrodynamic liposome diameter, see Experimental Procedures. The ψ_0 and ζ values are given for the liposomes without bound probes (see also text). The standard medium (pH 7.4) contained LUVET's with different PA contents as indicated, 0.5 mg of total lipid·mL^{-1}, and 2 μM probe. [b] ψ_0 estimated from measured ζ potential. [c] Could not be determined accurately.

hydroxycoumarins, and their essentially different interaction with the charged membrane (hydrophobic *and* electrostatic), probably govern the altered dissociation behavior.

As an alternative method to obtain a "standard" pK_a^0 and pK_a shifts we have also performed titrations in the presence of 20 mM Mg^{2+}, which is believed to screen the surface charges under the present conditions. At ψ_0 values down to −70 mV this method gives roughly the same pK_a^0 values, but at higher surface charge densities 20 mM Mg^{2+} may not be able to effectively screen these because the pK_a shifts increased less than expected. Moreover, at this Mg^{2+} concentration and at higher pH, vesicle aggregation was observed, severely hindering accurate fluorescence titrations.

The ψ_d and pH_d values calculated from the observed pK_a shifts are presented in Figure 7. These data are compared with the simulated ψ_d profiles as function of ψ_0 (Figure 7A). The simulated curves represent the ψ_d sensed at the distances (d) of the four fluorophores and at distance 0 nm. Figure 7B shows the data points for the four probes and the simulated curves for ψ_d and pH_d as function of distance from the membrane surface. The obtained values are in good agreement with the predictions over the applied ψ_0 range, provided that the adsorption of K^+ is taken into account.

Measurements of ζ Potentials. The ζ potentials were determined (Table I) in order to check if these go hand in hand with the calculated probe ψ_d values over the applied charge density range in the 400-nm LUVETs. In a ψ_d versus ψ_0 plot (not shown) the ζ potential data fit reasonably well to simulated curves for d = 0.6–0.7 nm, and roughly coincide with the data for U-6 (d = 0.64 nm). Therefore, we conclude that the probes produce realistic values, in good proportion to direct electrokinetic measurements.

Vesicle Size Measurements. Interestingly, the measured vesicle diameters were found to decrease with increasing PA fraction, i.e., negative surface charge density (Table I, upper section). Apparently, the curvature increase due to charge repulsion predominantly occurs in the outer bilayer leaflet. It should be mentioned that by the present method only average sizes are determined, not size distributions. We have also investigated a possible effect of vesicle size on the magnitudes of the measured interfacial potentials with U-6 (Table I, lower section). The smallest LUVETs exhibit slightly lower ζ potentials and pK_a values for U-6, as compared to the larger 10% PA LUVETs (upper section). Winisky et al. (1988) observed no significantly different ψ_d values, obtained from probe–quencher interactions, in vesicles with diameters of about 25 and 100 nm.

Experiments with Yeast Cells. Probe binding and fluorescence spectra showed similar characteristics as in LUVETs (data not shown). Addition of glucose at high initial pH to the starved cells (or a pH increase if glucose is already present) induces the well-known medium acidification down to pH 4–6, due to the extrusion of carboxylic acids and in part by energy-linked efflux of protons. This phenomenon was employed for "self-titration" experiments. Such a self-titration is illustrated by the recordings in Figure 8 for the probe U-6. After addition of 50 mM glucose the medium acidification starts and is almost complete in about 15 min, as monitored by the pH electrode. The midpoint of the probe fluorescence decrease is then used for the pK_a determination. Such measurements have been carried out with the four probes in the absence and presence of 20 mM $MgCl_2$. Unlike liposomes, yeast cells do not aggregate at this $MgCl_2$ concentration, and there is no alternative way to determine the pK_a shifts. The observed apparent pK_a values for U-2, U-6, U-10, and U-13 were in the absence of Mg^{2+} 9.29, 7.76, 8.88, and 7.89, respectively; in the presence of Mg^{2+} these values were 8.54, 7.20, 8.47, and 7.56. The respective pK_a differences then lead to the ψ_d values and corresponding pH_d values, shown in Figure 9. The ψ_0 potentials of various strains of yeast cells were earlier estimated to be about −60 mV, and the ζ potentials were found to be about −8 mV (Theuvenet et al., 1984). The estimated ψ_0 of −53 mV from the simulated profile with optimal fit to the four probe data points thus seems quite reasonable, when association of the medium Na^+ and K^+ is also taken into account. When the observed value for the ζ potential of 7.8 (±0.7) mV is placed on the curve, one could tentatively assume a distance for the plane of shear of about 2.6 nm, much larger than for the LUVETs (however, see Discussion).

DISCUSSION

This work shows that the new series of float-like fluorophores produces reliable values for the interfacial potential and pH at different surface potentials and distances. Over the applied ψ_0 range down to about −100 mV the data obtained with these probes and with the known probe U-2 fit remarkably well to

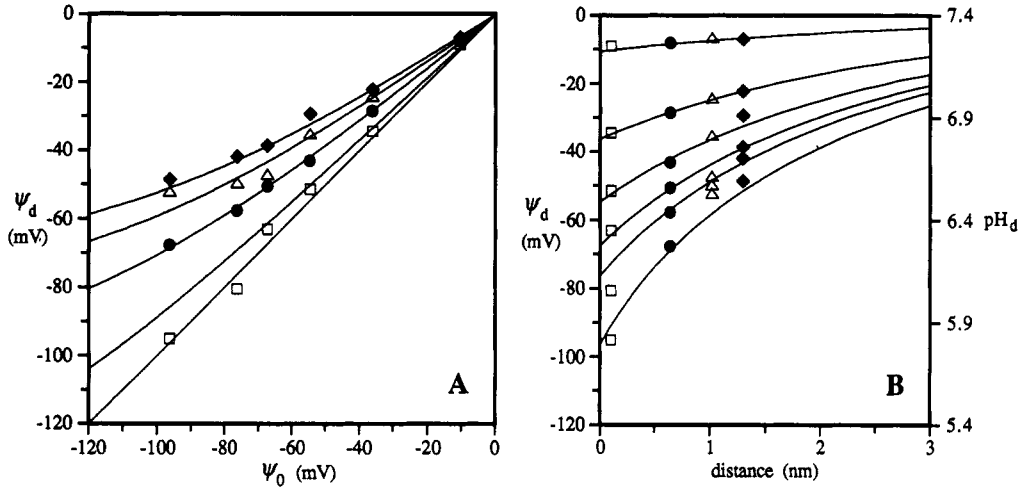

FIGURE 7: Interfacial potentials (ψ_d) obtained with the fluorescent probes as function of membrane surface potential (ψ_0), compared with the ψ_d curves, simulated for the assumed fluorophore distances from the membrane surface (A), and ψ_d and pH$_d$ as function of distance, compared with the corresponding simulations (B). In panel A the curves from bottom to top were simulated for d = 0, 0.2, 0.64, 1.02, and 1.30 nm, respectively. In panel B the initial ψ_0 potentials of the curves corresponds to those listed in Table I, upper section. Standard deviations of probe data varied between 3.5 and 7.7 mV (5–9 experiments). (□) U-2; (●) U-6; (△) U-10; (◆) U-13.

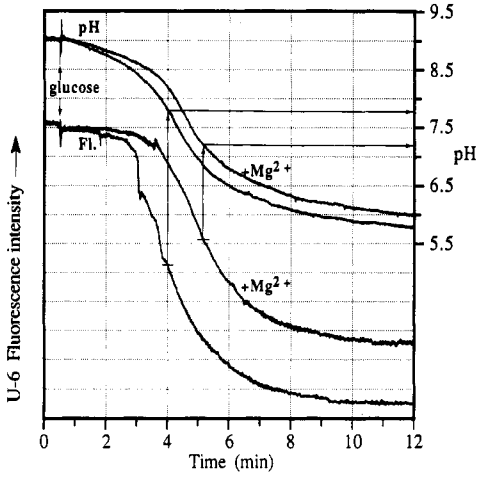

FIGURE 8: U-6 fluorescence and medium pH changes in starved yeast cells during glucose-induced medium acidification. The concentration of bound U-6 was 5 nmol·mg of protein^{-1}. For further details see Experimental Procedures.

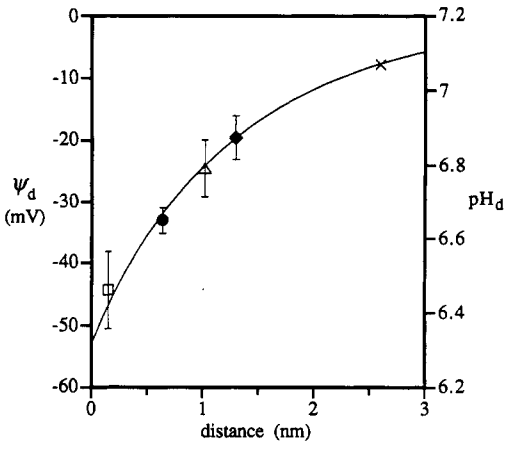

FIGURE 9: Interfacial potential (ψ_d) and pH (pH$_d$) values obtained with the fluorescent probes in yeast cells as function of distance from the membrane surface. The curve represents the ψ_d (or pH$_d$) profile simulated for the used monovalent salt concentration, pH$_b$ = 7.2 and ψ_0 = −53 mV. The observed value for the ζ potential (×) was placed on the curve to estimate the distance of the shear boundary. Probe data are means of 6–9 experiments.

the potential or pH profiles predicted by the (nonlinear) Gouy–Chapman theory (Figure 7). The corresponding ζ potentials are in good proportion to the probe data and follow roughly the same profile as U-6. It has been demonstrated by Eisenberg et al. (1979) and Ermakov (1990) that, apart from cation screening, accounted for in the Gouy–Chapman theory, adsorption of monovalent cations to lipid bilayers significantly affects the ψ_0 and ζ potentials. Obviously, cation adsorption must be taken into account although accurate and independent determination of the association constants is difficult. In our calculations an association constant (K_{as}) for K^+ of 1.6 (±0.5) M^{-1} (in 10 mM KCl) was used. Without correction (K_{as} = 0) the data are still fairly well covered by the simulated potential profiles in the lower charge density range, but at higher charge densities ($\psi_0 < -60$ mV) the simulations clearly indicate too negative potentials as compared to the observed probe data. Appreciable overall fits are obtained if K_{as} is varied between 1 and 2.

Winisky et al. (1988) and Langner et al. (1990) applied a variety of lipoid fluorescent and paramagnetic probes for the same purpose. Although the assumed fluorophore–membrane distances of these probes were not completely verified, their results are also in good agreement with predictions. Recently, Shin and Hubbell (1992) introduced a new approach based on the measurement of collision frequency of soluble with membrane-bound or macromolecule-bound nitroxide free radicals by electron–electron double resonance. For liposomes these authors also conclude excellent agreement of the electrostatic potential measurements with the Gouy–Chapman theory.

The proposed positioning of the probes normal to the membrane surface (Figure 1) is supported by their binding behavior and by the results from fluorescence anisotropy and quenching experiments. The distances between the fluorophores and the membrane surface may vary due to flexibility in the spacer groups, in particular of U-10 and U-13. In view of the proposed PC head-group structure and dynamics (Seelig et al., 1987; Scherer & Seelig, 1989; Macdonald et al., 1991; Makino et al., 1991), containing both PA and the float-like probes, it is likely that the PC dipole will stretch upward with the choline–N^+ away from the surface. The spacers of the embedded probes will also assume a stretched rather than a tilted orientation. Conversely, all probes, including U-2, will induce some perturbation of the head-group domain in their immediate vicinity. However, at the low probe concentrations

used, we did not observe a net change of surface charge, and there were no significant effects on proton translocation in yeast and chloroplasts (data not shown).

The binding characteristics of the float-like probes seem to be mainly governed by the electrostatic interaction between PA and the tetradecyl-bound quaternary ammonium group, although the contribution of the hydrophobic interaction to the binding is expected to be stronger. This additional electrostatic interaction will provide a better fixed fluorophore–membrane distance. Also in the case of diphenylhexatriene, a probe for the hydrocarbon domain fluidity, more consistent results were obtained after introduction of a quaternary ammonium group to anchor the probe in the head-group region (Prendergast et al., 1981). The positioning of the probe U-2 is probably less fixed, as suggested by the pH dependency of its rotational freedom (Figures 3 and 4) and accessibility to a cationic quencher (Figure 5B). The ψ_d data are obtained by titration in the high pH range at maximal mobility, and fit best to a distance of about 0.15 nm between its 7-hydroxyl group and the plane through the PA phosphoryl groups in the lipid head-group domain. The decreased mobility of U-2 at pH below 8 indicates that in this pH range its fluorophore is indeed more buried in the lipid head-group layer, as suggested by Pal et al. (1985) and Fromherz (1989).

This work also demonstrates that a series of well-defined liposomes, prepared by the extrusion method of Mayer et al. (1986) and containing different negative surface charge densities, offers a powerful model system to investigate membrane interfacial phenomena. Additional size measurements are important to check for the absence of vesicle aggregation and also because their size is significantly dependent on the surface charge density. Moreover, this would reveal the unwanted presence of large adhered probe micelles. In addition to the size measurements, the accessibility of the probes to various quenchers (Figure 5 and mentioned controls) excludes the presence of pure probe micelles under our experimental conditions.

Such a series of liposomes with varying surface charge also offers a unique possibility to estimate the distance of the plane of shear by entering the ζ data in ψ_d versus ψ_0 plots (cf. Figure 7A) and simulating the ψ_d profiles for different distances until a best fit to the data is obtained. The inherent assumption is that this distance is constant for smooth liposomes of varying size. In our particular case of PC/PA mixtures this would suggest a distance for the plane of shear of about 0.6–0.7 nm (at a K^+ association constant of 1.6 M^{-1}), which falls within the range suggested by Overbeek and Wiersema (1967) but is significantly larger than the more widely adopted distance of about 0.2 nm (cf. Eisenberg et al., 1979; Ermakov, 1990). However, in view of the complexity of interactions between PA, having two ionizable groups, and the PC head-group dipole (cf. Scherer & Seelig, 1989; Makino et al., 1991), and at the present stage of investigation, we are more than hesitant to claim that our estimation is correct. We are presently conducting a detailed study of the shear boundary position with various membrane types, including independent measurements of cation adsorption, using U-6 and other fluorescent probes.

In yeast cells (Figure 9) and chloroplasts (Kraayenhof et al., 1986) the observed ζ potentials are much lower compared to the estimated surface potentials than in smooth liposomes, which would imply larger distances for their shear boundaries. It is plausible to assume that this average distance may vary with the degree of membrane folding, particle size and shape, and the presence of large peripheral proteins, apart from other factors (cf. Overbeek & Wiersema, 1967). A large surface occupancy by proteins may also lower the ζ potential, without affecting the ψ_d values sensed by the probes. In that case the ζ potential is not indicative for the position of the plane of shear. The present uncertainties imply that ζ potentials measured in poorly characterized biomembranes should not be used for estimations of the actual surface potentials.

For further studies in liposome systems and applications in biomembranes the probe U-6 is recommended as the best choice. This probe allows consistent ψ_d measurements at d = 0.64 nm and more reliable estimation of ψ_0 than ζ potential measurements. It is also a promising tool to study dynamic properties of biomembrane interfaces. Its pK_a^0 is close to pH 7 and even small changes of interfacial potential and pH can be readily detected in the physiological pH range. In this respect it has great advantage over U-2 and similar probes. U-6 can be easily synthesized with high yield and to excellent purity as described here; it is stable and shows sufficient solubility in ethanol. Moreover, this probe provides the shortest possible membrane distance when combining a small fluorophore with an anchoring group. Like the other coumarins its fluorescence has a high quantum yield so that nonperturbing concentrations can be used. Even in highly pigmented membranes such as the thylakoids from chloroplasts these probes can be used despite of the unfavorable position of their excitation and emission maxima. Thylakoid-bound U-6 was found to monitor light-induced and uncoupler-sensitive fluorescence changes with much faster kinetics than the external medium pH changes. The application of U-6 for discrimination of bulk and interfacial proton displacements in chloroplasts and proteoliposomes is subject of present investigations.

ACKNOWLEDGMENT

Prof. Stuart McLaughlin is kindly acknowledged for constructive comments during this work and for critically reading the manuscript. We are also grateful to Prof. Ben de Kruijff, Dr. Hanneke Leenhouts, and Dr. Frits A. de Wolf for their valuable advice and materials for the preparation of well-defined LUVETs. Dr. Klaas Krab is acknowledged for providing very useful simulation programs and for frequent discussions. The help of Dr. Ronald W. Visschers and Dr. Frank van Mourik with the fast fluorescence measurements was indispensable.

REFERENCES

Borst-Pauwels, G. W. F. H., & Theuvenet, A. P. R. (1984) *Biochim. Biophys. Acta 771*, 171–176.

Davies, J. T., & Rideal, E. K. (1963) *Interfacial Phenomena*, 2nd ed., Chapter 2, Academic Press, New York.

De Kouchkovsky, Y. (1975) in *Proceedings of the 3rd International Congress on Photosynthesis* (Avron, M., Ed.) Vol. 2, pp 1013–1020, Elsevier, Amsterdam.

Eisenberg, M., Gresalfi, T., Riccio, T., & McLaughlin, S. (1979) *Biochemistry 18*, 5213–5223.

Ermakov, Y. A. (1990) *Biochim. Biophys. Acta 1023*, 91–97.

Fernández, M. S., & Fromherz, P. (1977) *J. Phys. Chem. 81*, 1755–1761.

Fromherz, P. (1973) *Biochim. Biophys. Acta 323*, 326–334.

Fromherz, P. (1989) *Methods Enzymol. 171*, 376–387.

Fromherz, P., & Masters, B. (1974) *Biochim. Biophys. Acta 356*, 270–275.

Grzesiek, S., & Dencher, N. A. (1988) *Biochim. Biophys. Acta 938*, 411–424.

Heberle, J., & Dencher, N. A. (1992) *Proc. Natl. Acad. Sci. U.S.A. 89*, 5996–6000.

Hubbell, W. L. (1990) *Biophys. J. 57*, 99–108.
Hubbell, W. L., & McConnell, H. M. (1971) *J. Am. Chem. Soc. 93*, 314–326.
Kraayenhof, R. (1970) *FEBS Lett. 6*, 161–165.
Kraayenhof, R. (1980) *Methods Enzymol. 69*, 510–520.
Kraayenhof, R., & Arents, J. C. (1977) in *Electrical Phenomena at the Biological Membrane Level* (Roux, E., Ed.) pp 493–504, Elsevier, Amsterdam.
Kraayenhof, R., De Wolf, F. A., Van Walraven, H. S., & Krab, K. (1986) *Bioelectrochem. Bioenerg. 16*, 273–285.
Kraayenhof, R., Schuurmans, J. J., Valkier, L. J., Veen, J. P. C., Van Marum, D., & Jasper, C. G. G. (1982) *Anal. Biochem. 127*, 93–99.
Krämer, R. (1989) *Methods Enzymol. 171*, 387–394.
Lakowicz, J. R. (1986) *Principles of Fluorescence Spectroscopy*, Chapter 6, Plenum Press, New York.
Langner, M., Cafiso, D., Marcelja, S., & McLaughlin S. (1990) *Biophys. J. 57*, 335–349.
Macdonald, P. M., Leisen, J., & Marassi, F. M. (1991) *Biochemistry 30*, 3558–3566.
Makino, K., Yamada, T., Kimura, M., Oka, T., Ohshima, H., & Kondo, T. (1991) *Biophys. Chem. 41*, 175–183.
Mayer, L. D., Hope, M. J., & Cullis, P. R. (1986) *Biochim. Biophys. Acta 858*, 161–168.
McLaughlin, S. (1977) *Curr. Top. Membr. Transp. 9*, 71–144.
McLaughlin, S. (1989) *Annu. Rev. Biophys. Biophys. Chem. 18*, 113–136.
Montal, M., & Gitler, C. (1973) *J. Bioenerg. 4*, 363–382.
Overbeek, J. T. G., & Wiersema, P. H. (1967) in *Electrophoresis* (Bier, M., Ed.) Vol. II, pp 152, Academic Press, New York.
Pal, R., Petri, W. A., Ben-Yashar, V., Wagner, R. R., & Barenholz, Y. (1985) *Biochemistry 24*, 573–581.
Penefsky, H. S. (1979) *Methods Enzymol. 56*, 527–530.
Prats, M., Teissié, J., & Tocanne, J. F. (1986) *Nature 322*, 756–758.
Prendergast, F. G., Haugland, R. P., & Callahan, P. J. (1981) *Biochemistry 20*, 7333–7338.
Rigler, R., Rabl, C.-R., & Jovin, T. M. (1974) *Rev. Sci. Instrum. 45*, 580–588.
Rouser, G., Fleischer, S., & Yamamoto, A. (1975) *Lipids 5*, 494–496.
Rubin, B. T., & Barber, J. (1980) *Biochim. Biophys. Acta 592*, 87–102.
Schapendonk, A. H. C.M., Hemrika-Wagner, A. M., Theuvenet, A. P. R., Wong Fong Sang, H. W., Vredenberg, W. J., & Kraayenhof, R. (1980) *Biochemistry 19*, 1922–1927.
Scherer, P. G., & Seelig, J. (1989) *Biochemistry 28*, 7720–7728.
Schlieper, P., Medda, P. K., & Kaufmann, R. (1981) *Biochim. Biophys. Acta 644*, 273–283.
Seelig, J., Macdonald, P. M., & Scherer, P. G. (1987) *Biochemistry 26*, 7535–7541.
Shin, Y.-K., & Hubbell, W. L. (1992) *Biophys. J. 61*, 1443–1453.
Soucaille, P., Prats, M., Tocanne, J. F., & Teissié, J. (1988) 289–294.
Teissié, J., Prats, M., Soucaille, P., & Tocanne, J. F. (1985) *Proc. Natl. Acad. Sci. U.S.A. 82*, 3217–3221.
Thelen, M., Petrone, G., O'Shea, P., & Azzi, A. (1984) *Biochim. Biophys. Acta 766*, 161–168.
Theuvenet, A. P. R., Van De Wijngaard, W. M. H., Van De Rijke, J. W., & Borst-Pauwels, G. W. F.H. (1984) *Biochim. Biophys. Acta 775*, 161–168.
Torres-Pereira, J. M. G., Wong Fong Sang, H. W., Theuvenet, A. P. R., & Kraayenhof, R. (1984) *Biochim. Biophys. Acta 767*, 295–303.
Träuble, H., & Eibl, H. (1974) *Proc. Natl. Acad. Sci. U.S.A. 71*, 214–219.
Van Walraven, H. S., Marvin, H. J. P., Koppenaal, E., & Kraayenhof, R. (1984) *Eur. J. Biochem. 144*, 555–561.
Waggoner, A. S., & Stryer, L. (1970) *Proc. Natl. Acad. Sci. U.S.A. 67*, 579–589.
Winiski, A. P., Eisenberg, M., Langner, M., & McLaughlin, S. (1988) *Biochemistry 27*, 386–392.